Optimization of ships in shallow water with viscous flow computations and surrogate modeling

Rotteveel, Erik; van der Ploeg, A; Hekkenberg, Robert

Publication date
2016

Document Version
Final published version

Published in
Proceedings of the 13th International Symposium on Practical Design of Ships and Other Floating Structures

Proceedings of PRADS2016
4th – 8th September, 2016
Copenhagen, Denmark

Optimization of ships in shallow water with viscous flow computations and surrogate modeling

Erik Rotteveel[1)], Auke van der Ploeg [2)] and Robert Hekkenberg [3)]

[1)]Delft University, Netherlands
[2)] Maritime Research Institute Netherlands (MARIN), Netherlands
[3)] Delft University, Netherlands

Abstract

Shallow water effects change the flow around a ship significantly which can affect the optimum design of the hull. This paper describes a study into the optimization of the aft ship region for various water depths. The research focuses on variations of the following parameters of a hull form: The athwart ship's propeller location, the tunnel top curvature, the flat-of-bottom shape in the stern region and the stern bilge radius. All hull form variants are evaluated in 3 different water depths using a viscous flow solver, and a surrogate model is created for each water depth. Pareto plots are used to present the trade-off between the optimization for one or another water depth. Finally, specific hull forms are chosen and the differences in flow behavior among hull forms and water depths are explained.

Keywords

Hull form optimization; computational fluid dynamics; inland ships; shallow water.

Introduction

Due to shallow water effects, optimization of inland ships is more complex than that of sea-going ships. In shallow water, the ship's nominal resistance, the thrust deduction and the wake fraction will in general increase. The close relation between the hull form design and the exact amount of increase in each of these parameters in shallow water makes the optimization of inland ships extra challenging. A ship that is optimal for deep water may not be optimal in shallow water. Moreover, the water depth an inland ship encounters can change numerous times along the route. For each change of water depth, the ship's speed also changes because of regulations, or because critical speeds or large squat effects have to be avoided. Therefore, a *range* of water depths and ship speeds, rather than a *single* depth and speed, should be considered during inland ship optimization.

In this paper, we focus on the optimization of the aft part of an inland ship. While model tests play an important role in ship optimization, they are costly in terms of budget and time, especially if multiple hull forms are to be investigated. Computational Fluid Dynamics (CFD) allows for cheaper analysis of a ship for multiple parametric variations and operating points. Therefore, CFD is chosen as analysis tool for this study. Reynolds-Averaged Navier-Stokes (RANS) solvers are used, since potential flow solvers omit viscous effects which are important in the aft ship region. Furthermore, all hull form evaluations will be done at full-scale Reynolds numbers.

We will investigate the effects of the parameters considered on the ship's resistance, wake fraction and power, as well as the effect that water depth has on the optimal choice of these parameters.

Hull forms are generated from a parametric model with input generated from a Latin Hypercube Design. We will discuss some computed trends and differences in those trends depending on the water depth. A surrogate model is built from the computational results (Scholcz et al, 2015). The quality of the surrogate model is tested by cross-validation. The model is used to approximate the optimal ship for typical water depths encountered during the operation of an inland ship. For the optimal ships, flow visualizations are used to explain why these ships are optimal.

Hull Form Parameterization

The first step is to define hull form parameters and to generate hull forms. To do this, Rhinoceros 3D is used. A parametric hull form model is set up that allows for the variation of the following four parameters: the athwart ship's propeller position, the shape of the flat of bottom in the stern region, the bilge radius in the stern region and the shape of the tunnel top. A tunnel geometry is a typical shallow-water ship feature to prevent ventilation in case of limited draft. The following four images provide an example of a variation of each parameter:

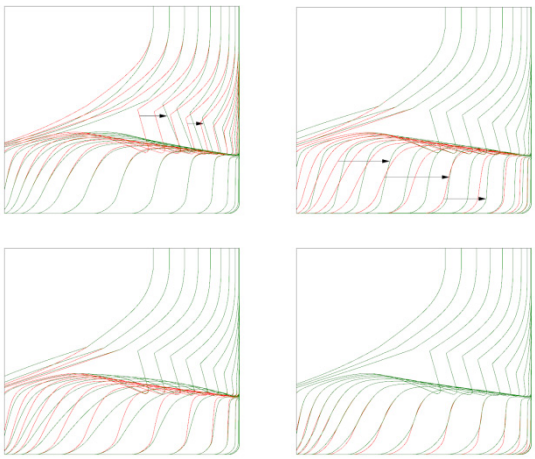

Figure 1. Demonstration of the parameters. From left to right and top to bottom: Athwart ships propeller position (Yprop), Flat-of-bottom shape (Vbottom), Tunnel Top Curve (Aroof) and bilge radius (Rbilge)

The choice of parameters is based on prior knowledge from earlier publications (Rotteveel, 2015; vd Meij, 2013; Heuser, 1986) and on earlier results from the Top Ships project. This project aims to improve design knowledge regarding inland ships. The chosen parameters turned out to have a significant influence on ship resistance, the propeller wake field and propulsion power. The parameter range is chosen such that the hull form changes significantly, yet remains realistic.

Design Of Experiments

A set of 50 different ships was generated from a *Latin Hypercube Design (LHD)*. This type of design was chosen because it limits the number of required computations (denoted by N) while it is still space-filling. Suppose that the number of parameters is denoted by n. According to (Wang, 2003) the saturation level for a LHD would be $N = \frac{(n+2)(n+1)}{2}$, whereas a full factorial approach would require 3^n samples. Given the current set of parameters, these formulas yield 15 and 81 experiments respectively, showing that the LHD is much more efficient.

Evaluation Approach

Each of the involved hull form variants is analyzed using the viscous flow solver PARNASSOS (Hoekstra, 1999). This solver has a solution technique that is very efficient with respect to both CPU-time and memory usage (van der Ploeg et al, 2000), which makes it very well suited for doing systematic variations or combination with an optimization strategy (van der Ploeg et al, 2010). It computes the steady, turbulent flow around ship hulls by solving the discretized Reynolds-averaged Navier-Stokes equations for steady, incompressible flow. It is a finite-difference method and around the ship block-structured, HO-type body-fitted grids are used with a very strong contraction in wall-normal direction towards the hull in order to have y^+-values below 1 near the wall, even for full-scale computations. Double-body computations are used, since we assume that the influence of free-surface in the area where the chosen variations are most effective is small.

The inflow boundary is located $0.65L_{pp}$ in front of the bow, and the outflow boundary at $1.8L_{pp}$ behind the transom. Due to symmetry considerations, only the starboard side is taken into account. In an (x,y,z)-coordinate system fixed to the ship, with symmetry at $y=0$, x positive aft and z upward, the outer boundary is defined by $y=1.3L_{pp}$. At this boundary, tangential velocities and pressure found from a potential-flow computation are imposed. Since that computation gives good results already for much of the wave pattern, these boundary conditions (although of Dirichlet type for the pressure) hardly cause any wave reflection.

We will use two object functions: (Eq. 1) an estimate of required propulsion power and (Eq. 2) a function that describes the uniformity of the water flow towards the propeller. The first object function is an estimate of the power delivered to the propulsor:

$$P_D = \frac{R_T \times (1-w)}{1-t} \times \frac{V_S}{\eta_R \times \eta_0} \tag{1}$$

in which R_T is the towing resistance, w the estimated effective wake fraction, V_s the ship's speed, t the thrust deduction coefficient, η_o the propeller efficiency in open water, and η_R the relative rotative efficiency. The latter is approximated by 1, while η_o is obtained from the Ka-series of ducted propellers (Oosterveld, 1974). For each hull form, R_T, and $\eta_H=(1-t)/(1-w)$ are required to perform this evaluation. To compute t, we also perform a second RANS computation including a force distribution representing the propeller with an imposed thrust T_0 which is in the neighborhood of the thrust T required for self-propulsion, such that we can assume a linear behavior of the force on the hull as a function of the imposed thrust. The thrust deduction coefficient can then be computed from $t=(R_0-R_T)/T_0$, in which R_0 is the resistance force resulting from the second RANS computation.

As a second object function, we propose a norm of the variation of the full-scale wake. In case of danger of erosive cavitation, one would like to prevent strong variations of the wake in circumferential direction, especially in the top half of the propeller plane. We will use the L1-norm of the variation of the undisturbed propeller inflow angle

$$\beta = \tan^{-1}\left(\frac{V_x}{\omega\frac{r}{R} - V_\theta}\right) \tag{2}$$

with V_x and V_θ the axial and tangential velocity components respectively, θ the angular position in rad. and ω the propeller rotation rate in rad/s. The variation of β in circumferential direction as the propeller rotates is $\partial\beta/\partial\theta$. The L1-norm is determined from integration over the propeller plane..

The evaluation of the objective functions must be numerically accurate, as otherwise the predicted trends are

polluted or spoilt by numerical errors. In (van der Ploeg, 2013) it is shown that with the grid density we use, the grid dependence in the computed trends is only limited.

Results Analysis

Figures 2 and 3 show the comparison for computed propulsion power (Eq. 1) for two different water depths. From Figure 2, it is clear that the correlation between power in deep water (h/T = 3.0) and medium water depth (h/T = 2.0) is strong, and that an optimal ship in deep water probably is an optimal ship for a h/T value of 2.0 as well.

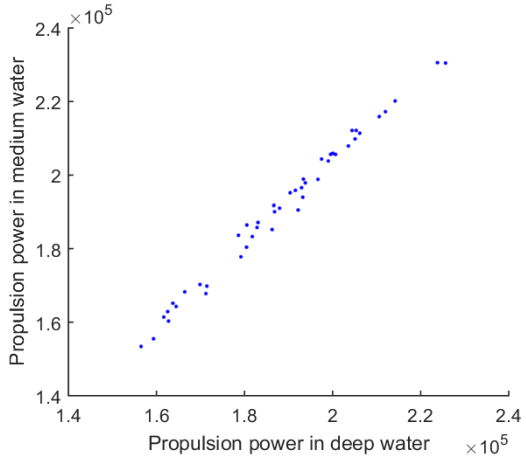

Figure 2. Propulsion power [W] in deep water (h/T = 3.0) against that in medium (h/T = 2.0) water depth

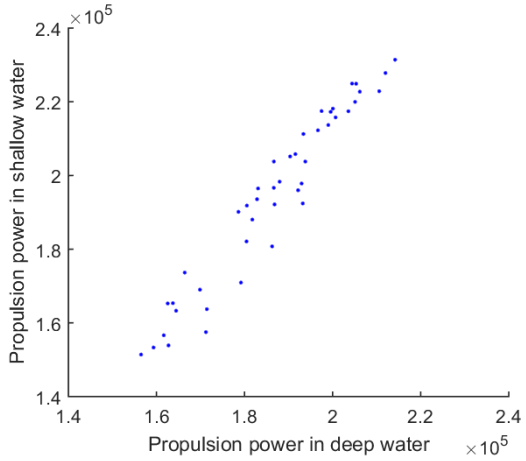

Figure 3. Propulsion power [W] in deep water (h/T = 3.0) against that in shallow (h/T = 1.5) water

Although it is weaker, this correlation is also present in Figure 3. The increased scatter is due to shallow water effects. The scatter would have been even larger in case a smaller water depth would have been investigated. The change of flow behavior causes that a ship that is optimal for deep water, can be less optimal for shallow water. This can be seen in the center of the graph; a ship with a higher power requirement in deeper water, actually has a lower (relative to the other ship) power requirement in shallower water. The increased scatter can be shown using the data variance as well. Table 1 shows the variance for propulsion power in all three water depths.

Table 1. Variance for power for three water depths

Water depth	Variance in P_D (σ^2)
h/T = 3.0	$2.988 \cdot 10^8$
h/T = 2.0	$3.909 \cdot 10^8$
h/T = 1.5	$6.350 \cdot 10^8$

Table 2. Variance for resistance for several water depths

Water depth	Variance in R_T (σ^2)
h/T = 3.0	$2.93 \cdot 10^5$
h/T = 2.0	$2.59 \cdot 10^5$
h/T = 1.5	$2.02 \cdot 10^5$

The increasing dependence of propulsion power on the parameters is opposite to what happens to resistance. For resistance, the data variance decreases with decreasing water depth, as shown in Table 2. This effect can also be seen in Figure 4. There, the increase factor for resistance in shallow water is plotted against deep water resistance. A trend can be observed that a ship with low deep water resistance has a larger increase of resistance for shallow water, thereby flattening the variance in the dataset and thus reducing parameter effects on resistance. This is contrary to what has been observed in (Raven, 2016). This apparent contradiction may be explained by the fact that the present study focuses on hull form details for a single ship type whereas in (Raven, 2016), entirely different ship types were analyzed in shallower water than considered in this paper.

Despite the fact that in shallower water the resistance becomes less dependent on the chosen parameters , the variance for both the wake fraction and thrust deduction increase in shallower water, as shown in Table 3. Meanwhile, variance for propeller efficiency is reduced. Despite that, the increase of variance for wake and thrust deduction is sufficiently large to lead to the observed increase of variance for required propulsion power.

Table 3. Variance in w, t and η_0 for varying depths

Water depth	Var(w)	Var(t)	Var(η_0)
h/T = 3.0	2.96E-03	2.27E-04	2.35E-04
h/T = 2.0	3.99E-03	2.80E-04	2.11E-04
h/T = 1.5	7.16E-03	5.09E-04	1.33E-04

From Figures 2 and 3, an additional observation can be made: in the lower-left region, some cases show a smaller power requirement in shallow water than in deep water. This seems unrealistic, and can probably be explained by the fact that omitting the free surface leads to part of the increased resistance being ignored, while the increase of wake fraction and thrust deduction are not significantly affected by the absence of the free surface. Then, from (Eq. 1) it follows that the hull efficiency increases, leading to a lower power requirement in shallow water. However, it is reasonable to assume that the analysis of trends is not affected by this phenomenon, since the parameters do not affect the waterline geometry and therefore the interaction between wave resistance and the chosen parameters is small.

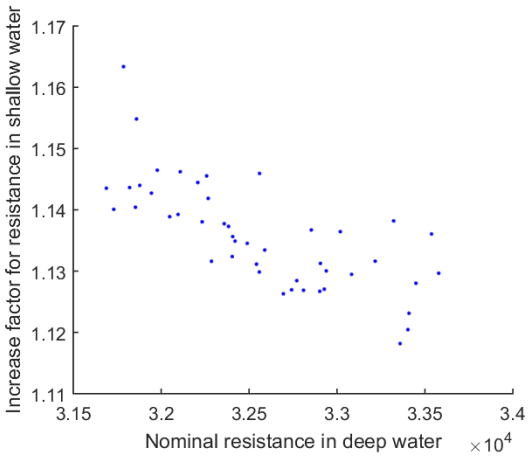

Figure 4. Increase factor for nominal (no propeller effect) resistance from deep (h/T = 3.0) to shallow (h/T = 1.5) water.

Response Surface Generation

Based on the results, response surfaces are generated in three ways: Kriging, quadratic and universal Kriging. The quality of these surfaces is analyzed using cross-validation, where a surface is constructed based on $N-1$ results, while the value of the *N-th* result that has been left out is compared to the prediction at the same location. This same approach has been used by (Kim et al, 2011) and gives a quick view of the response surface quality. Furthermore, the Root Mean Squared Error can be estimated. Based on these evaluations, we will make a choice for a response surface that will be used for further steps in the present study.

Table 4. Relative error values for response methods

Response surface type	RMSE Value
Quadratic	0.0881
Kriging	0.1194
Universal Kriging	0.0891

RMSE values are shown in Table 4, and cross-validations are presented in Figure 5. The quadratic response surface shows the best behavior, although the universal Kriging method is close. Therefore, the quadratic response surface is used for further analysis. Both methods involving Kriging are relatively sensitive to small distortions in the data, resulting in locally large deviations between observations and predictions. In addition to Figure 5, Figure 6 shows the quadratic response surface cross-validation for h/T = 2.0 and 1.5, providing a similar pattern as that for h/T = 3.0. Since the general trends are linear, it is concluded that the response surface approximates the real response sufficiently accurate.

Response Surface Analysis And Application

Which parameters contribute the most to the variance in power requirement can be determined from an Analysis of Variance (ANOVA). ANOVA determines the change of variance in the model if one of the parameters is removed from the model. Figure 7 shows ANOVA results for different water depths. From the graph, it is clear that the parameter Yprop is the most important parameter in all cases; while Vbottom is second. Compared to these two parameters, the remaining parameters (Rbilge and Aroof) are less relevant.

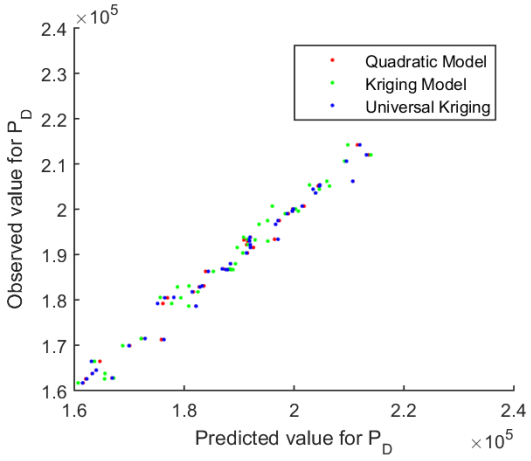

Figure 5. Cross-validation between observations and response surface predictions for h/T = 3.0

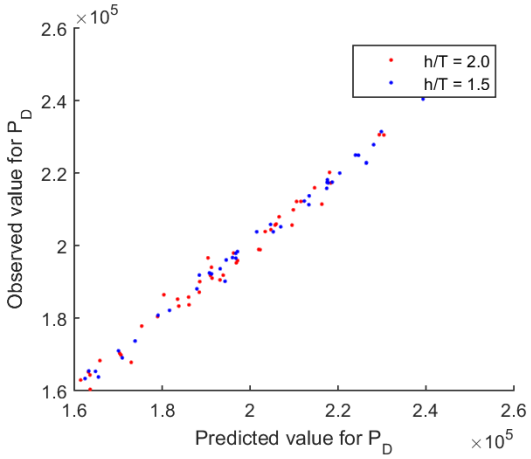

Figure 6. Cross-validation for h/T = 2.0 and 1.5

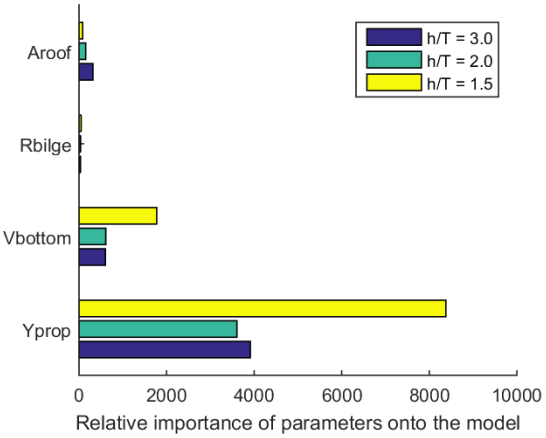

Figure 7. ANOVA graph, showing the relative importance of parameters on power requirement.

According to Figure 7, the Yprop parameter becomes increasingly important with decreasing water depth. The same applies to Vbottom. An opposite effect can be observed for Aroof; its importance decreases in shallow water. This may be due to the parameter range for Aroof being set around the optimum for a small water depth, since that would lead to relative small variance due to that parameter.

Figure 7 provides useful information on which parameter is important to vary to improve an inland ship for its power requirement. However, it does not necessarily show *how* each of the parameters influences the power requirement.

This can be investigated using the response surfaces. Comparing two ships in our dataset would not be sufficient, since multiple variables change between any two ships due to the use of a LHD. Figures 8 to 11 show the behavior of the two most important parameters (Yprop and Vbottom) in the dataset. In Figure 8 and 9, the power requirement is plotted against the parameter value of one of the two parameters, for multiple values of the other parameter. The values for power requirement are determined from the response surface. The remaining two parameters were set at their medium value.

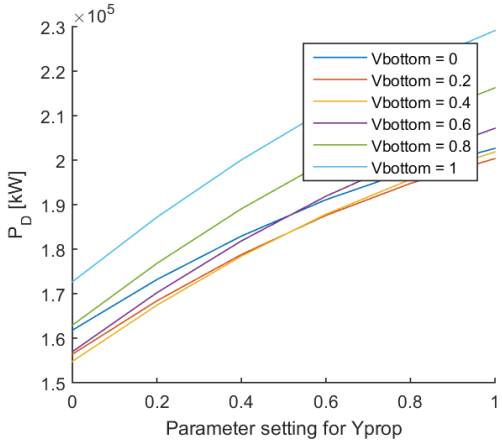

Figure 8. Power prediction versus Yprop and Vbottom (isolines), for h/T = 3.0

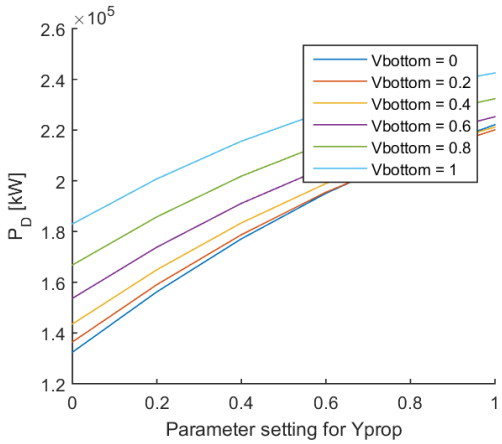

Figure 9. Power prediction versus Yprop and Vbottom (isolines), for h/T = 1.5

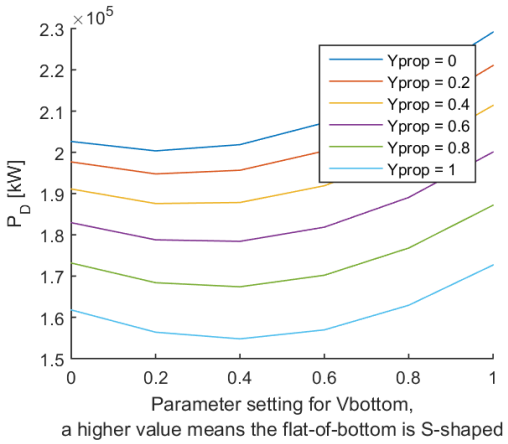

Figure 10. Power prediction versus Vbottom (x-axis) and Yprop (isolines), for h/T = 3.0

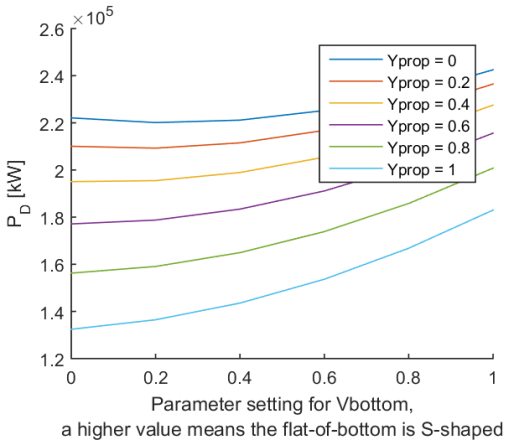

Figure 11. Power prediction versus Vbottom (x-axis) and Yprop (isolines), for h/T = 1.5

Figures 8 to 11 show that a smaller value for Yprop (hence a propeller closer to the centerplane) leads to a lower power requirement. This can be attributed to the stronger wake field present near the centerplane, leading to higher propeller efficiency. For low values of Vbottom (which means a single-curved flat-of-bottom) the gradient of power versus Yprop decreases, but a propeller closer to the centerline remains better in terms of efficiency. Figures 10 and 11 show that the value of Vbottom can be chosen optimal. Furthermore, a strongly S-shaped flat-of-bottom seems not favorable, as the optimum is on the low side of Vbottom.

Figures 10 and 11 also show that the optimal choice for Vbottom shifts at shallow water. The optimum moves towards a fully V-shaped hull. An explanation for this is that at shallow water, more inflow into the propeller comes from aside the ship. If the flat-of-bottom is S-shaped, strong curvature of streamlines in the horizontal plane can occur, leading to higher resistance.

At this point, it is clear which parameters most significantly affect the power requirement of the ship, and also how the influence of these parameters behaves in different water depths. In order to investigate how the optimal design differs for shallow water, the generated response surfaces are used to determine the power requirement if the displacement is constrained at 3890 tons. For each

hull form evaluated, Figure 12 presents the shallow water requirement against that for deep water. The figure shows that the trade-off between these water depths is practically absent. Probably, shallow water effects are that strong yet at h/T =1.5. It thus appears that, given the parameters and their variation as studied in this paper, an optimal ship for relatively shallow water can be obtained through optimization at deep water.

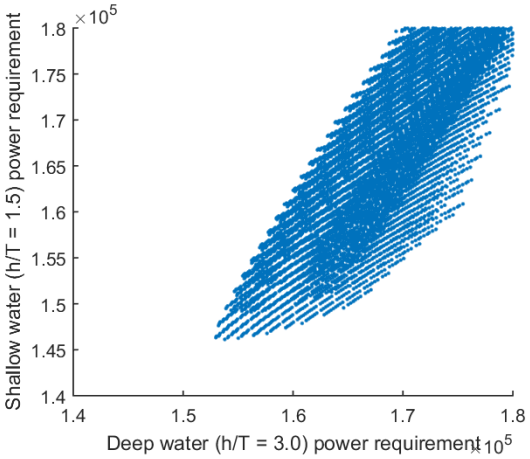

Figure 12. Data points from response surface evaluations for h/T = 3.0 and h/T = 1.5, limited to a displacement of 3890 tonnes.

Another trade-off usually made is that between propeller efficiency and the wake object function. The trade-off here is that a stronger wake field leads to a better propeller efficiency but usually comes at the cost of increased variations in the propeller blade angle of attack. The trade-off between ship power requirement and the wake object function (WOF) is presented for all three water depths in Figure 13. The trade-off between power requirement and the WOF is clear: a lower power requirement leads to a stronger variation of propeller inflow. This trade-off does not significantly change with water depth, leading to a similar conclusion as obtained from Figure 12: a hull form that is optimal in deep water (for the parameters investigated), is optimal in shallow water as well.

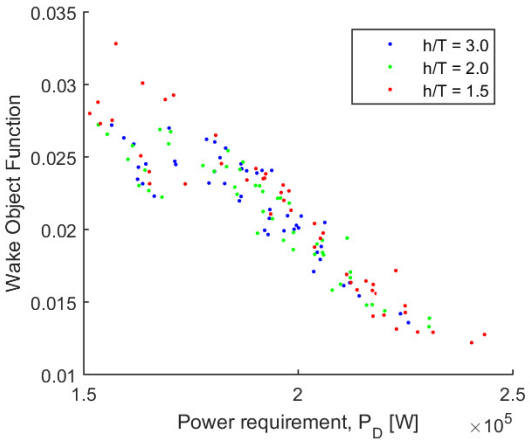

Figure 13. Pareto plot for power requirement and wake object function

For the parameters considered, it thus appears that one may achieve an optimal hull form using optimization in deep water already. Figure 14 illustrates this. The pictures show the longitudinal flow in the propeller plane for three different water depths. Although there are differences between h/T = 3.0 and h/T = 1.5, these mainly relate to the magnitude of velocities. The change of flow behavior is not yet sufficient to shift the optimal design to another point in the design space.

Together with Figure 15, Figure 14 also provides an explanation for the importance of the athwart ships position of the propeller (Yprop). Both Figures show a strong wake near the ship center. For the ship in Figure 14, the propellers are operating partly inside this wake, yielding a better hull efficiency due to a larger wake fraction and a lower power requirement. Meanwhile, the vortices being shed from the tunnel skirt are smaller for the ship in Figure 15. Due to this, the resistance of the ship in Figure 15 is approximately 3.5 percent lower compared to that in Figure 14. This indicates that it is important to always taken into account effects on propulsion if one is optimizing a ship. Also, it indicates that a separate treatment of the tunnel skirt and athwart ships position of the propeller is interesting.

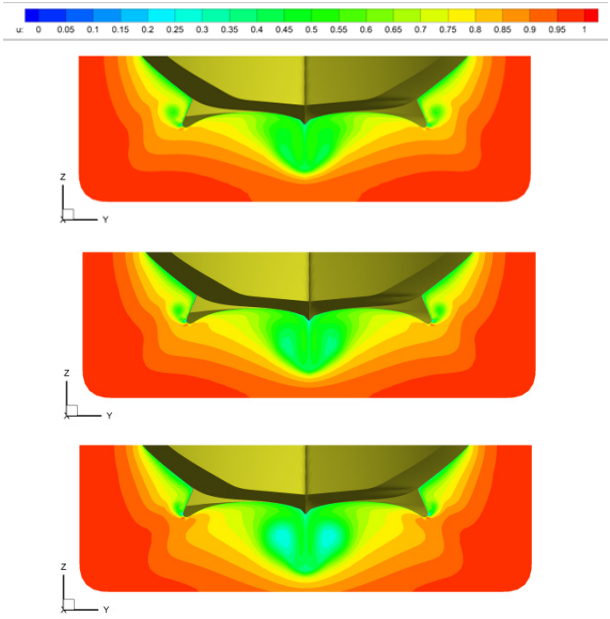

Figure 14. Velocity profile at the propeller plane for three different water depths. Top to bottom: h/T = 3.0, h/T = 2.0 and h/T = 1.5.

Another observation from Figure 14 is that the vortex shed from the tunnel skirt becomes smaller with decreasing water depth. We could reason that in very shallow water, a tunnel geometry converging towards the aft of the ship can be profitable in terms of resistance. For the water depths presently investigated, this effect does not yet occur.

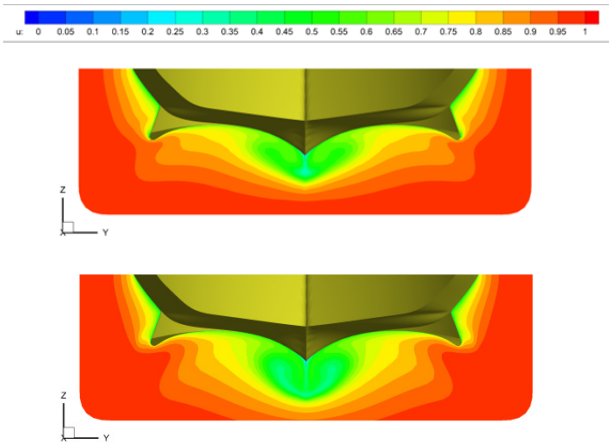

Figure 15. Velocity profile at the propeller plane, for a ship with the propellers located far away from center, for h/T = 3.0 (top) and h/T = 1.5 (bottom).

From Figure 7 it follows that the shape of the flat-of-bottom in the stern is important as well. Figure 16 shows the velocity distribution at the propeller plane for a ship with similar characteristics to the ship in Figure 14, but with an S-curved flat-of-bottom. Due to this hull form modification, the wake fraction decreases, as does the thrust deduction since the distance between the propeller and the skeg geometry increases. Resistance increases as well, in total leading to a power increase of 5 percent in deep water, and 7 percent in shallow water. However, the WOF decreases by 14 and 15 percent respectively.

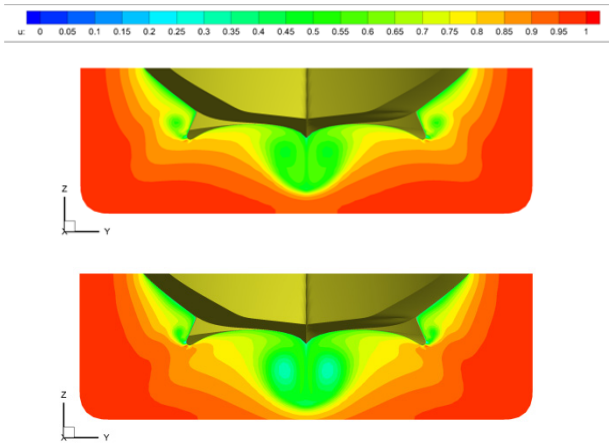

Figure 16. Velocity profile at the propeller plane for the ship with smallest athwart ships propeller position, for h/T = 3.0 and h/T = 1.5.

Figure 17 shows the limiting streamlines, comparing the ships from Figures 16 and 14. The explanation for the improved wake field is seen in the limiting streamlines, which converge at the skeg for the top image. This indicates the separation of vortices. These vortices are convected into propeller disk, increasing the wake object function. For the other ship, the streamlines follow the bilge towards the end of the skeg, without converging into a vortex separation point. Therefore, despite the ship from Figure 14 being optimal in terms of power, the wake quality may be improved by a modification to the curvature of the flat-of-bottom.

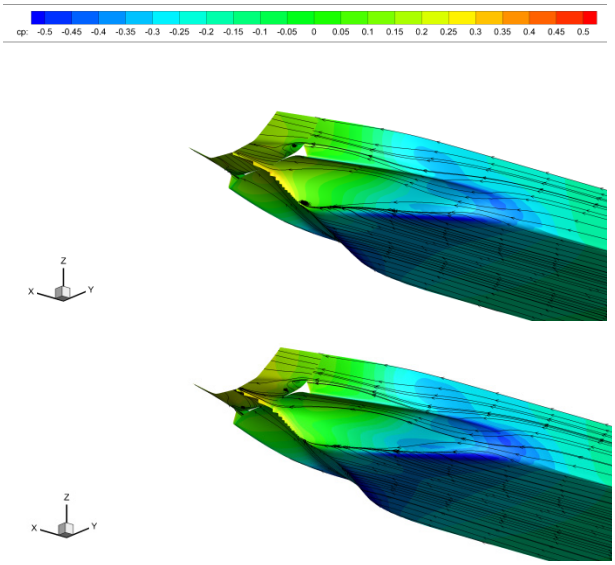

Figure 17. Pressure distribution for ships from Figures 14 (top) and 16 (bottom). Limiting streamlines are also presented. h/T = 1.5 for both cases.

For the remaining two parameters, the effects on power requirement are smaller. The curvature of the tunnel top affects thrust deduction and resistance in opposite direction, therefore having no significant effect on power.

For the bilge radius, the effect is notable for resistance, but it also reduces the wake fraction and therefore its effect on powering is limited again. The wake object function is also mostly affected by the propeller position and the flat-of-bottom curvature. The first parameter moves the propeller in or out of the region where the wake is strongest, while the second affects the point of vortex separation.

Conclusions

Double-body computations have been performed for 50 different inland ships, for which the stern region was varied using four parameters. Various types of response surfaces were created, of which a quadratic response surface shows the best agreement with the results from the computations. Using this response surface, it was found that two of four parameters show a much larger influence on the power requirement than the others. Furthermore, the response surfaces were used to investigate whether the optimal design point for the hull form would change in shallow water.

This change was not observed for the parameters and water depth investigated in the present study. For h/T = 1.5, the shallow water effects are not severe enough to significantly affect the flow behavior. Therefore, the ship that is, in terms of power, optimal in deep (h/T = 3.0) water is also optimal for shallow water. For the wake object function (WOF), we observed similar results: the trade-off between the WOF or required power does not change significantly for h/T = 1.5. This is interesting, since h/T ratios lower than 1.5 might not occur that often, hence might not be worth optimizing a ship for. Given the presented results, it appears that optimization for deep water can be sufficient. Still, it

would be interesting to investigate a smaller water depth as well, for example h/T = 1.2.

We have shown the effect of the propeller position on required power and the WOF. The tunnel skirt, moving along with the propeller, sheds a smaller vortex when moved away from the center plane, leading to lower resistance. However, the propeller is then also moved to an area where the ship's wake is weaker. Therefore, the effect on the required power can be opposite to that on resistance. On the other hand, a propeller operating (partly) inside the ship's wake leads to an increase of the WOF, leading to a higher risk of cavitation or nuisance. A treatment where the propeller position is separated from the tunnel skirt position would be interesting.

Furthermore, in Figure 14, we have shown that the optimal choice for this parameter could be affected by water depth if a lower h/T ratio would be considered: smaller vortices are shed in shallow water.

The shape of the flat-of-bottom affects thrust deduction since the ship's geometry is further away from the propeller for an S-shaped bilge line. At the same time, resistance increases, and the wake fraction slightly decreases. Overall, the effect of this parameter on the required power is smaller than for the effect of the propeller position. Meanwhile, the flat-of-bottom shape affects vortex shedding from the bilge, thereby having a significant effect on the wake object function. A slightly S-shaped bilge line reduces the WOF significantly.

The other parameters involved had a negligible effect on the power requirement. The curvature of the tunnel top shows an effect on nominal resistance, which is partly compensated by an increase of thrust deduction.

References

Van Brummelen, EH, Raven, HC and Koren, B (2001). "Efficient numerical solution of steady free-surface Navier-Stokes flow," Jnl. Computational Physics, Vol. 174, pp. 120-137.

Heuser, H. (1986). "Verdrangungschiffen auf Flachem Wasser," Schiffstechnik, Vol. 33 (1), pp 20-48.

Hoekstra, M (1999). "Numerical simulation of ship stern flows with a space-marching Navier Stokes method," Thesis, Technical University of Delft.

Hoekstra, M and Raven, HC (2003). "A practical system for hydrodynamic optimization of ship hull forms," NAV 2003 Conference, Palermo, Italy.

Kim, H, Jeong, S, Yang, C and Noblesse, F (2011), "Hull form design exploration based on response surface method," Proceedings 21st Int. Offshore and Polar Engineering Conference, Hawaii, USA.

Menter, FR (1997). "Eddy-viscosity transport equations and their relation to the k-ε model," Journal of Fluids Engineering,Vol. 119, pp. 876-884.

Oosterveld, MWC (1970), "Wake adapted ducted propellers," Dissertation, Delft University of Technology, Delft.

Raven, HC, Van der Ploeg, A and Starke, AR (2004). "Computation of free-surface viscous flows at model and full scale by a steady iterative approach," 25th Symp. Naval Hydrodynamics, St.John's, Canada.

Raven, HC (2016). "A new correction procedure for shallow-water effects in ship speed trials," Kopenhagen, Denmark.

Rotteveel, E. and Hekkenberg, RG. (2015) "The influence of shallow water and hull form variations on inland ship resistance," Proceedings 12th IMDC, Tokyo, Japan.

Van der Ploeg, A and Hoekstra, M (2009). "Multi-objective optimization of a tanker after body using PARNASSOS," Proceedings 12th NuTTs-symposium, Cortona.

Van der Ploeg, A, Hoekstra, M and Eça, L (2000). "Combining accuracy and efficiency with robustness in ship stern flow computation," Proc. 23rd Symp. Naval Hydrodynamics, Val de Reuil, France.

Van der Ploeg, A and Raven, HC (2010). "CFD-based optimization for minimal power and wake field quality," Proceedings 11th International Symposium on Practical Design of Ships and other Floating Structures, Rio de Janeiro, pp. 92-101.

Van der Ploeg, A and Raven, HC, Starke, AR and Veldhuis, C. (2013), "Optimization of a chemical tanker with free-surface viscous flow computations," Proceedings 12th International Symposium on Practical Design of Ships and other Floating Structures, Changwon City, Korea, pp. 716-723.

Scholcz, TP, Gornicz T. and Veldhuis C., (2015), "Multi-objective hull-form optimization using Kriging on noisy computer experiments," International Conference on Computational Methods in Marine Engineering, Rome.

Van der Meij, KH and Raven HC, (2014), "Promising hydrodynamic improvements for inland vessels," Proceedings EIWN Conference, Budapest, Hungary.

Van der Ploeg, A , (2015), "RANS-based optimization of the aft part of ships including free surface effects," International Conference on Computational Methods in Marine Engineering, Rome.

Wang, GG, (2003), "Adaptive response surface methods using inherited Latin Hypercube Design points," Journal of Mechanical Design, Vol. 125, pp 210 – 220.